Available online at www.sciencedirect.com

ScienceDirect

Ceramics International 40 (2014) 73–80

CERAMICS INTERNATIONAL

www.elsevier.com/locate/ceramint

Template-free fabrication of pure single-crystalline $BaTiO_3$ nano-wires by molten salt synthesis technique

Bao-rang Li*, Wei Shang, Zhong-liang Hu, Nai-qiang Zhang

The National Thermal Power Engineering Technology Research Center & Key Laboratory of Condition Monitoring and Control or Power Plant Equipment, North China Electric Power University, Beijing 102206, China

Received 16 April 2013; received in revised form 28 May 2013; accepted 28 May 2013
Available online 15 June 2013

Abstract

Large amounts of $BaTiO_3$ nano-wires have been produced by the molten-salt synthesis method. Powder X-ray diffraction, field emission scanning electron microscopy, and transmission electron microscopy were used to investigate structure and morphology of the obtained products. Moreover, the current work also proposes synthesis mechanism of $BaTiO_3$ nano-wires when barium nitrate and titanium dioxide were chosen as starting materials. The results revealed that the dissolution rate of the initial precursors was a critical factor refining the shape of the final products. An impedance-type humidity sensor was finally fabricated based on as-prepared $BaTiO_3$ nano-wires and tested with humidity performance providing that $BaTiO_3$ nano-wire is suitable for high-performance humidity sensors.

Keywords: A. Powders: solid state reaction; D. $BaTiO_3$ and titanates; E. Sensors

1. Introduction

Perovskite-phase metal oxides exhibit a variety of interesting physical properties including ferroelectric, dielectric, pyroelectric, and piezoelectric behavior. Among these metal oxides, $BaTiO_3$ is an important material and has been widely used in multilayer ceramic capacitors (MLCC), chemical sensors, and nonvolatile memories, due to its attractive dielectric and ferroelectric characteristics.

One-dimensional (1D) structured materials, such as nanotubes, nano-rods, nano-wires, and nano-ribbons, etc., have attracted widespread attentions because of their potential applications. In order to fabricate low dimensional nanostructures, a significant number of methods have been developed over the past decades. In general terms, these methods can be approximately separated into two groups. The first and the earliest process is molten-salt synthesis (MSS). The second process is the wet chemical process with or without a template [1–4]. The wet chemical methods usually have some disadvantages, such as complicated synthetic routes and high synthetic cost. But, the MSS method is a relatively simple method to prepare ceramic powders, in which a molten salt is used as a reaction medium for reactant dissolution and precipitation. So, MSS has been widely used to synthesize functional 1D structured oxide ceramics. For example, Wang et al. reported that high-purity CoO nano-wires were synthesized by MSS and at the same time their optical properties were also investigated [5]. By optimizing reaction temperature, time and weight ratio of the precursors to KCl salt, Lan et al. synthesized a large amount of $K_6Ta_{10.8}O_{30}$ nano-wires [6]. In order to avoid the complex synthesis process, Deng et al. prepared single-crystalline $BaTi_2O_5$ nano-wires using the mixed KCl–NaCl as salt fluxes [7].Using a modified multi-step molten salt method, Santulli et al. fabricated one-dimensional $LiNbO_3$ with gram quantities successfully [8]. Depending upon the same synthesis route, Liu et al. synthesized YVO_4:Ln (Ln = Eu^{3+}, Dy^{3+}) nano-phosphors [9]. Recently, this technique has been found to be used to prepare many new types of nano-materials, such as SiC, mullite and titanium nitride nano-wires, etc. [10–12]. Due to its distinguishing features, MSS is also applied to synthesize $BaTiO_3$

*Corresponding author. Tel.: +86 010 61772355; fax: +86 010 61772383.
E-mail address: libr@ncepu.edu.cn (B.-r. Li).

0272-8842/$ - see front matter
http://dx.doi.org/10.1016/j.ceramint.2013.05.105

with 1D nanostructure. For example, Hayashi et al. reported the synthesis of rod-shaped $BaTiO_3$ particles in the molten chloride by using rod-shaped $TiO_2 \cdot nH_2O$ and $BaCO_3$ as precursors [13]. Mao et al. produced single-crystalline $BaTiO_3$ nano-rods and $SrTiO_3$ nano-particles by using barium or strontium oxalate and TiO_2 as the staring materials [14]. Deng et al. obtained 1D nano-structured $BaTiO_3$ by using a surfactant-free approach in a non-aqueous molten salt media [15]. In the same year, Huang et al. reported the synthesis of morphology-controlled $BaTiO_3$ nanostructures such as spherical, cube-shaped and rod-shaped $BaTiO_3$ from a reaction of $BaO/BaCO_3$ and TiO_2 with a eutectic mixture of NaCl–KCl flux at 700 °C for 1 h [16]. These investigations indicate $BaTiO_3$ particles morphologies are usually influenced greatly by the sizes and shapes of the precursor particles (such as TiO_2). So, in most cases, in order to prepare $BaTiO_3$ nano-wires with cubic or pseudocubic crystal structure, a possible strategy is to use the rod-shaped reactant, which usually has a low solubility in the salt, as template [17]. However, Deng et al. reported the first preparation of perovskite $BaTiO_3$ nano-strips in a molten salt without using any surfactant and templates. They attributed the $BaTiO_3$ nano-wires formation to the symmetry breaking from self-polarize along the aggregation axis [15]. These investigations suggest although much work has been done on the synthesis of perovskite nanostructures, the control of nucleation and growth of 1D nanostructure materials is still a big challenge because the $BaTiO_3$ 1D nanostructure is difficult to obtain because of the isotropy of the $BaTiO_3$ tetragonal crystal structure and the anisotropy of the 1D structure. So, in this paper, the MSS method was used to fabricate $BaTiO_3$ nano-wires and large-scale single-crystalline $BaTiO_3$ nano-wires were successfully synthesized in a molten salt without using any templates. Based on the experimental results, the possible formation and growth mechanisms were further suggested. Moreover, $BaTiO_3$ humidity sensor was also fabricated and the nano-wires' humidity sensitivity property was characterized.

2. Experimental section

2.1. Sample preparation

The starting materials used in this experiment were analytical grade reagents. Barium nitrate ($Ba(NO_3)_2$) was mixed with titanium dioxide (TiO_2) at a molar ratio of 1:1. Then the mixture was mixed with KCl salt at a mass ratio of 1:10, and ground for 2 h in water solution to guarantee sufficient mixing uniformity. After proper ball-milling, the mixture was put in drying oven at 70 °C for 15 h. The dried mixture was then transferred into corundum crucibles and calcined at different temperatures for 4 h. When the crucible was cooled down to room temperature by furnace cooling, samples were collected and washed with deionized water to guarantee no ions left in the samples. Then the samples with deionzed water were dried in drying oven at 80 °C for 12 h. In order to selectively remove smaller nano-particles and nano-rods, the samples were disposed with centrifugation before humidity sensitivity test.

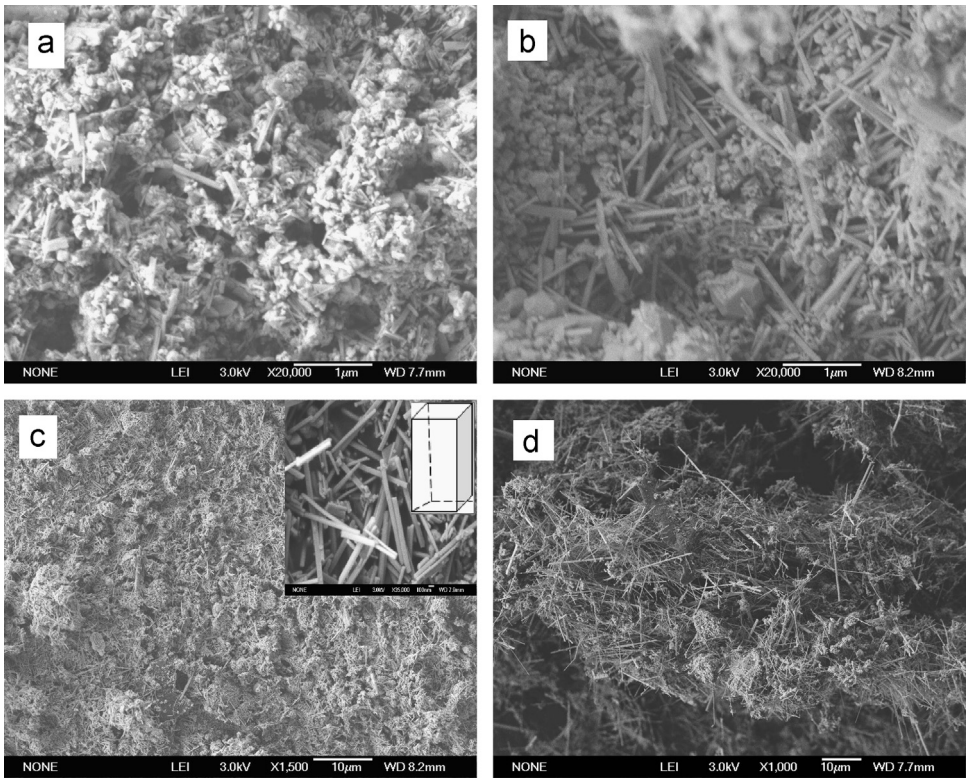

Fig. 1. SEM images of $BaTiO_3$ nano-wires synthesized by MSS, (a)750 °C; (b) 800 °C; (c) 850 °C and (d) 950 °C. Both the ball-milling time and holding time are 4 h.

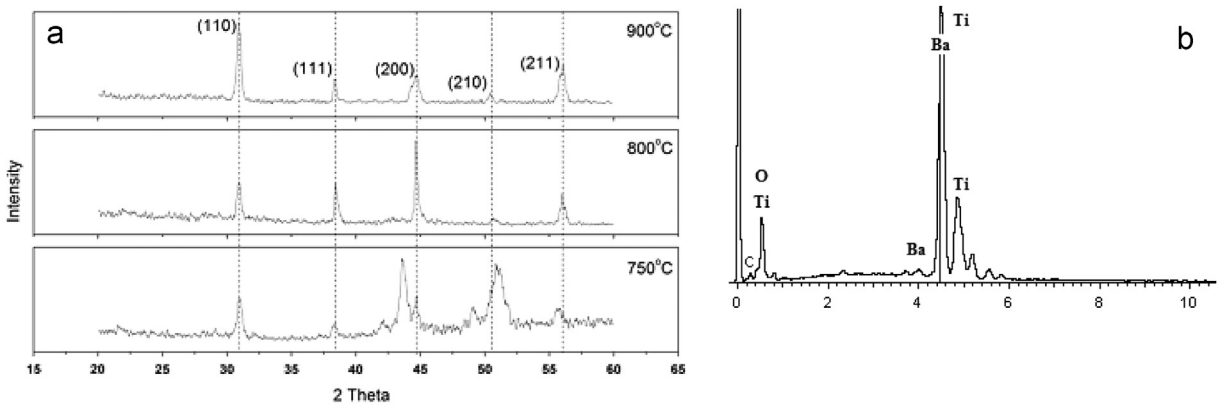

Fig. 2. XRD (a) and EDS (b) results of as-prepared BaTiO3 nano-wires.

2.2. Measurements

The phase and the purity of the as-prepared powder were characterized by X-ray diffraction (XRD), using Cu Kαradiation. The morphologies which included sizes and shapes of the prepared nano-particles were measured by scanning electron microscope (SEM, Model JSM-7401, JEOL, Japan) with an energy-dispersive X-ray spectrometer (EDS). For TEM observations, the $BaTiO_3$ nano-wires were ultrasonically dispersed in ethanol and then dropped onto carbon-coated copper grids. Then the structure of the sample was characterized by transmission electron microscope and high-resolution transmission electron microscope (HRTEM), which were performed on a JEOL JEM-2010 microscope.

In order to study its humidity sensing properties, the as-prepared nano-wires were mixed with deionized water to form a paste. The paste was dip coated on a ceramic substrate (6 mm × 3 mm, 0.5 mm thick) with five pairs of Ag–Pd interdigitated electrodes (electrodes width and distance: 0.15 mm) to form a sensing film dried in air at room temperature for 12 h. Finally, the humidity sensor was obtained after aging at 95% relative humidity (RH) with a voltage of 1 V, 100 Hz for 24 h to improve stability and durability. Controlled humidity environments were obtained with saturated salt solutions in a closed glass vessel. The humidity sensitivity test was done by a ZL-5 intelligent LCR analyzer (made in Shanghai, China) at room temperature.

3. Results and discussion

3.1. Characterization

The effect of growth temperature on the morphology of the products is investigated firstly. Fig. 1 shows the SEM images of the samples synthesized at different temperatures. When the reaction temperature is lower than 850 °C, pure $BaTiO_3$ nano-wires cannot be obtained. Fig. 1(a) is the SEM image of the products prepared at 750 °C, showing that the product is composed of small particles and micro-sized rods. Furthermore, the product is not pure phase $BaTiO_3$ as shown in the XRD pattern (see Fig. 2). $BaTiO_3$ nano-wires are synthesized at 850 °C. It can be found from Fig. 1(c) that the product mainly consists of a large amount of straight nano-wires. The diameters of the nano-wires are in the range of 30–100 nm as shown in the high magnification SEM image (inset of Fig. 1 (c)). The surfaces of the nano-wires are smooth which revealed the possibility of single crystalline characterization in the nano-wires. When the reaction temperature is higher than 850 °C, for example 900 °C, the morphology of $BaTiO_3$ nano-wires does not change. But the length of the nano-wires increases to several tens micrometers (see Fig. 1(d)).

The purity and crystallinity of the as-synthesized samples are further examined by the powder XRD technique. The XRD patterns of the $BaTiO_3$ products obtained at different temperatures are shown in Fig. 2(a). At 750 °C, peaks corresponding to perovskite $BaTiO_3$ have begun to appear, but the peaks are ill-defined due to the low crystallinity of this phase. The well crystallization phase of $BaTiO_3$ is obtained in the samples treated at temperatures higher than 800 °C. All the intense diffraction peaks can be perfectly indexed to the cubic phase of $BaTiO_3$ according to JCPDS no. 31-0174. The composition of the nano-wire is subjected to energy-dispersive X-ray spectroscopy (EDS) analysis and the result is shown in Fig. 2(b). EDS characterization shows that the body of the nano-wire is exclusively composed of Ba, Ti and O with the ratio of Ba to Ti approximately equal to 1:1, conforming to the chemical formula of $BaTiO_3$.

The as-prepared $BaTiO_3$ product is further investigated by TEM. A representative TEM image of the $BaTiO_3$ nano-wires is shown in Fig. 3(a). It can be seen that the nano-wires have widths ranging from 30 nm to 100 nm and lengths reaching > several micrometers, in good agreement with the SEM results. The enlarged TEM images corresponding to points A and B shown in Fig. 3(a) are shown in Fig. 3(b and c), respectively. It is easily observed that the tops of the nano-wires are not all flat and some are obvious triangle or circular arc in shape, which is totally different from the reports and might imply a different growth mechanism. The HRTEM image of a single $BaTiO_3$ nano-wire (shown in Fig. 3 (d)) exhibits clear lattice fringes, indicating a high crystallinity of the nano-wire. The lattice spacings of 0.4013 and 0.1795 nm are recognized and can be ascribed to the (100) and (210) planes of the cubic phase of $BaTiO_3$, respectively. The nano-wire growth direction is seen to be along [001]. The selected-area electron diffraction (SAED) pattern in Fig. 3(e) also indicates that the nano-wires preferentially grow along the *c*-axis.

3.2. Effects of precursors on $BaTiO_3$ nano-wire formation

In order to investigate the possible influences of precursors on the synthesis of $BaTiO_3$ nano-wires, $BaTiO_3$ nano-wires were prepared by molten salt synthesis process, using $BaCl_2$, $Ba(NO_3)_2$, $Ba(CH_3COO)_2$, $BaCO_3$ and $Ba(OH)_2$ as precursors. Fig. 4 shows the morphologies of the $BaTiO_3$ powders obtained from the five precursors. It can be easily found from Fig. 4 that the precursors have significant effects on the nano-wires formation. Large quantity of micro-wires can be synthesized from $Ba(CH_3COO)_2$ precursor in spite of containing less amounts of spherical particles. The length of the obtained nano-wires can reach up to several tens of microns and the diameter is arranged from several nano-meters to about 500 nm. Fig. 1(c) shows typical nano-rods with the length–diameter ratio about 10 can be synthesized from $Ba(NO_3)_2$ precursor. However, for $Ba(OH)_2$ precursor, Fig. 4(e) indicates only less amounts of wire-like products can be synthesized under the same conditions. Fig. 4(a and d) suggests no obvious nano-wires are synthesized when $BaCl_2$

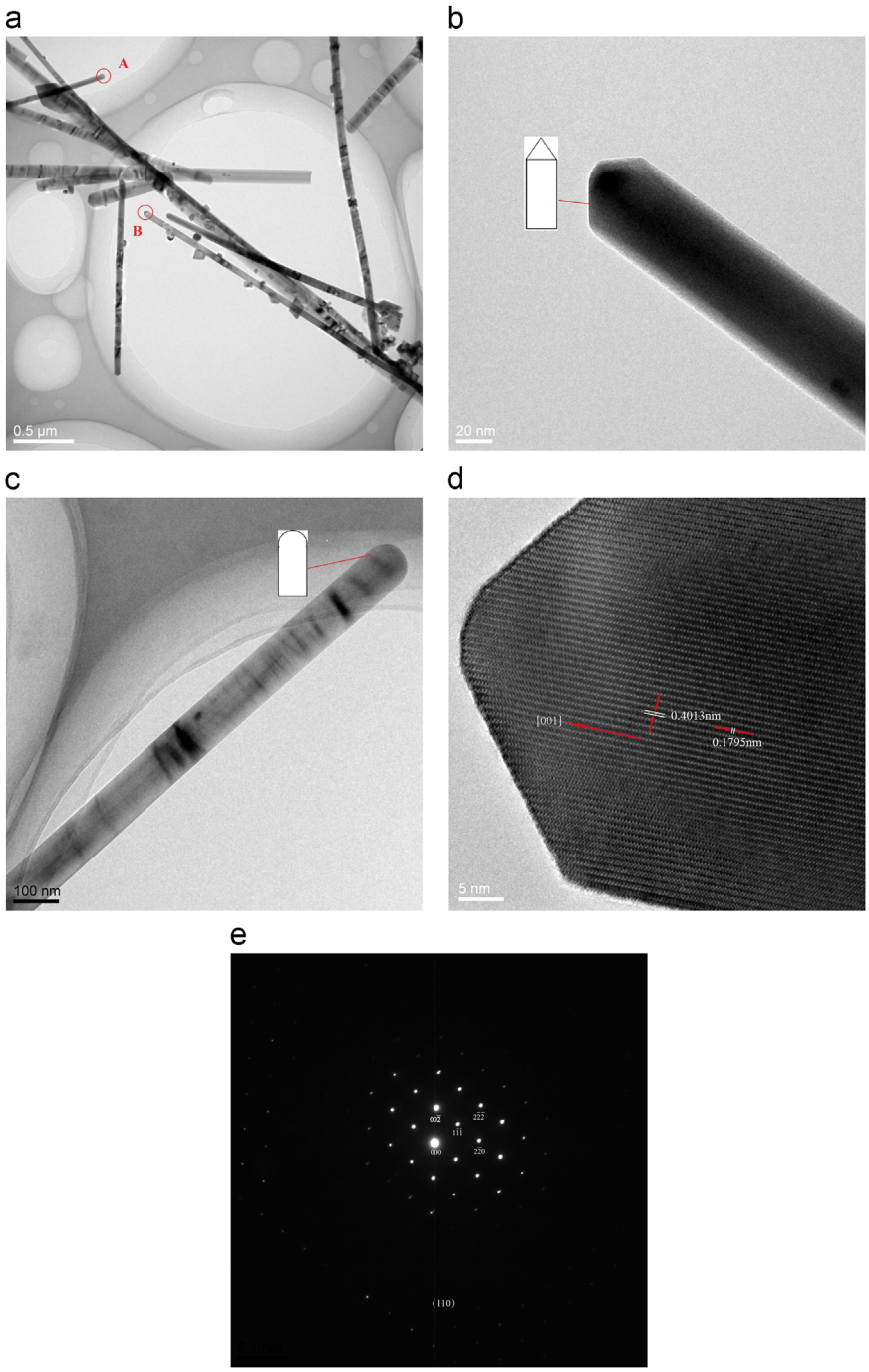

Fig. 3. (a) TEM image of as-prepared $BaTiO_3$ nano-wires; (b) the enlarged TEM image of part B shown in Fig. 3(a); (c) the enlarged TEM image of part A shown in Fig. 3(a); (d) HRTEM image of (b) and (e) SAED pattern of as-prepared single $BaTiO_3$ nano-wire.

and $BaCO_3$ are chosen as the precursors. In order to make further observations on the shapes and surface qualities of the formed nano-wires, the high magnification SEM images of the nano-wires are given in the insets of Fig. 4(c and e), respectively. For $Ba(CH_3COO)_2$ and $Ba(OH)_2$ precursors, obvious attachments can be found on the surfaces of the synthesized nano-wires. But for $Ba(NO_3)_2$ precursor, the surfaces of the nano-wires are shown to be very smooth which reveals the possibility of single crystalline characterization. Moreover, the enlarged SEM images also indicate the cross section shapes of the nano-wires obtained from different precursors are different. For $Ba(CH_3COO)_2$ precursor, it is obviously hexahedral in shape. But they are typical tetrahedral for both $Ba(OH)_2$ and $Ba(NO_3)_2$ precursors. These observations further confirm the influences of different precursors on the $BaTiO_3$ nano-wires formation.

3.3. Possible synthesis mechanism

Fig. 5 shows DSC and TG derivative curves of the mixed precursors measured at a heating rate of 10 °C/min. Three typical peaks can be observed in Fig. 5(a). The peak around 310 °C should have close relations to anatase–rutile phase transformation of TiO_2, which is consistent to the report [18]. The second peak around 770 °C is obviously due to the melt of potassium chloride while the third peak around 934 °C can be attributed to the formation of $BaTiO_3$. So, when the temperature is higher than 770 °C, the fast weight loss rate shown in Fig. 5(b) must be originated from both the formation of $BaTiO_3$ and decomposition of barium nitrate. Based on the experimental data shown in Fig. 5, the possible synthesis mechanism of $BaTiO_3$ nano-wires is discussed below.

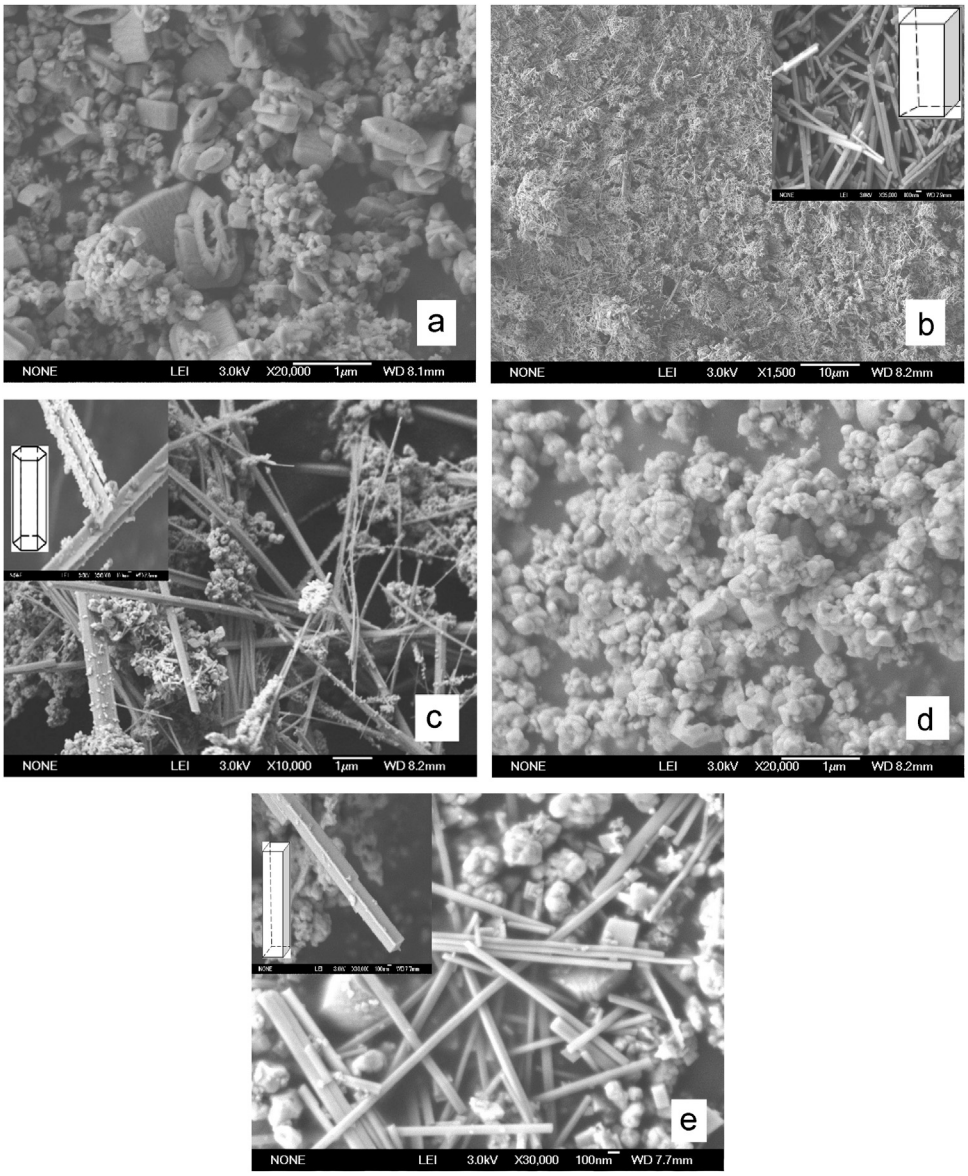

Fig. 4. SEM pictures of the $BaTiO_3$ nano-wires synthesized by MSS using different precursors. The calcinations temperature is 850 °C while the holding time is 4 h. (a) $BaCl_2$; (b) Fig. 1(c); (c) $Ba(CH_3COO)_2$; (d) $BaCO_3$ and (e) $Ba(OH)_2$.

In our studies, both barium nitrate and potassium chloride can be dissolved in deionized water. So after ball-milling, titanium dioxide particles were enwrapped by uniformly distributed molecules of barium nitrate and potassium chloride because titanium dioxide cannot be dissolved in deionized water. The melting point of barium nitrate is very low (depending upon the purity) and so it would melt and decompose gradually with temperature increasing. At the elevated temperature approaching to 770 °C (the melting point of potassium chloride), the materials enwrapping titanium dioxide particles would change to be barium oxide and potassium chloride. So, the synthesis reactions are probably happened as below:

$$2H_2O + 2Ba(NO_3)_2 \rightarrow 2Ba(OH)_2 + 4NO_2\uparrow O_2\uparrow$$
$$Ba(OH)_2 \rightarrow BaO + H_2O\uparrow$$
$$BaO + TiO_2 \rightarrow BaTiO_3$$

When the calcinations temperature is higher than 770 °C, potassium chloride starts to melt and at the same time barium oxide starts to be dissolved in potassium chloride. The solubility of barium oxide can be affected by many factors, such as temperature, time, amounts and types of salts, etc. So, the followed $BaTiO_3$ particles morphologies evolution would go along two directions, which are shown in Fig. 6. In the first flow of the proposed schematic diagram, for relatively low temperature and small ratios of the salt to the precursors, imperfect dispersion of both barium and titanium oxide particles cannot be avoided in spite of the ball-milling. Under these conditions, the agglomerated particles can slow the dissolved rate of barium oxide in salt. Finally, the left barium oxide in the precursors resulting from the limited solubility or slow dissolved rate can react with titanium oxide and synthesize $BaTiO_3$ particles directly by particle–particle contact, which is very similar to that of normal solid-state mechanism. In this case, no wire-like products can be formed. In the second flow of the proposed schematic diagram, for relatively high temperature and large ratios of the salt to the precursors, barium oxide has a high solubility and so large amounts of barium oxide can be dissolved in the molten salts. During the solution- precipitation process of barium oxide, the insoluble titanium oxide particles with sphere-like shape have chance to reunite into rods-like particles in the molten salt environment, which can be used as templates for further growth [19]. Under these conditions, the dissolved barium oxide can diffuse to the surfaces of rod-like titanium oxide and react in situ to synthesize $BaTiO_3$ nano-rods. It is worth mentioned that the above referred mechanisms do not work alone and in most cases they occur simultaneously in the synthesis process. So, both the particles and wires are usually presented together in the final synthesized products [Fig. 3(a)]. The influences of different precursors on the amounts of wire-like products might be due to different solubility of barium salts in potassium chloride. For obtaining large amounts of pure nano-wires, the effective controls on the synthesis parameters, such as temperature, time, amounts and types of salt, etc., become necessary.

On the basis of the above studies on the formation of $BaTiO_3$ nano-rods, a plausible mechanism for further growth of $BaTiO_3$ from nano-rods to nano-wires can be proposed in Fig. 7. The growth process of nano-wires with triangle tops may flow as follows with a number of key steps. First, the formed barium titanate nano-rods in the molten salt would be reunited in a certain way in order to reduce the surface energy and result in barium titanate crystal seeds (Fig. 7 step 1). Second, the aggregated

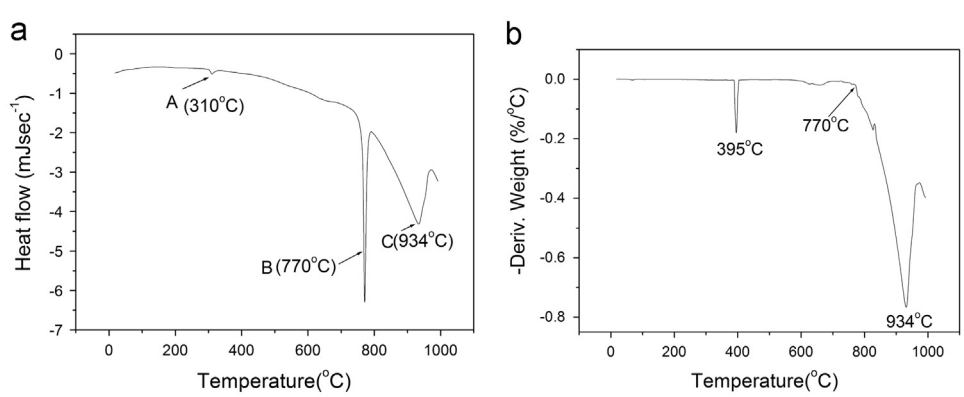

Fig. 5. (a) DSC and (b) TG derivative curves of the mixed starting materials.

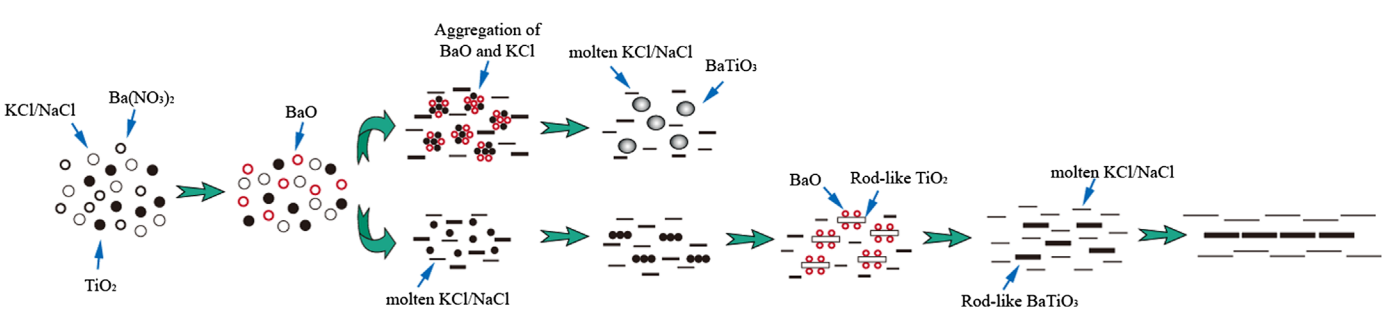

Fig. 6. Proposed schematic diagram of the synthetic mechanism of $BaTiO_3$ nano-rods.

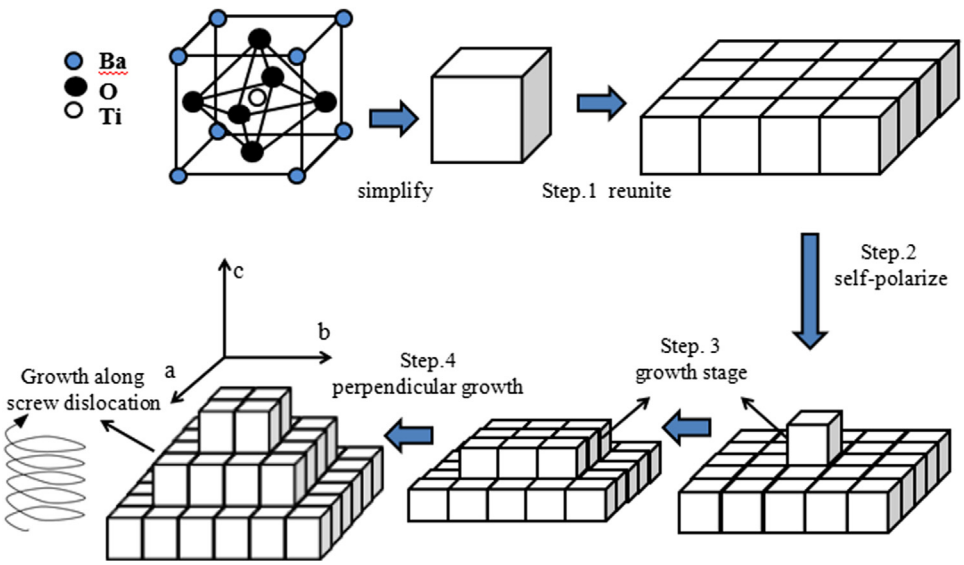

Fig. 7. Proposed schematic diagram of the growth mechanism from nano-rods to nano-wires.

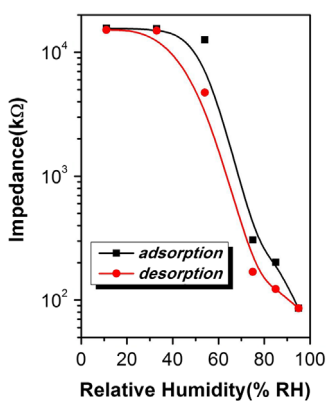

Fig. 8. Humidity hysteresis characteristic, the test condition was AC 1 V, 100 Hz.

perovskite crystal seeds would be apt to attract new nano-rods by self-polarize along *c* direction (the growth direction, Fig. 7 step 2) and simultaneously lead to the formation of the crystal growth stages in the corner parts between the contacted rods (marked by arrows) [15]. Depending upon these stages, the necessary energy for the further growth can be reduced effectively. So, these stages will attract new nano-rods continuously and result in growth along *b* or *a* direction, which is perpendicular to the growth direction. The competition between the two directional growth (*a* (or *b*) direction and *c* direction) finally brings about a spiral growth, which contribute to the formation of the nano-wires with a triangle top.

3.4. Humidity sensing properties

Fig. 8 shows the humidity hysteresis characteristic of the nano-sensor by keeping the applied voltage at 1 V and the frequency at 100 Hz. The black line stands for the course from low to high RH, corresponding to the absorption process, while the red line stands for the opposite direction, corresponding to the desorption process. The complex impedance

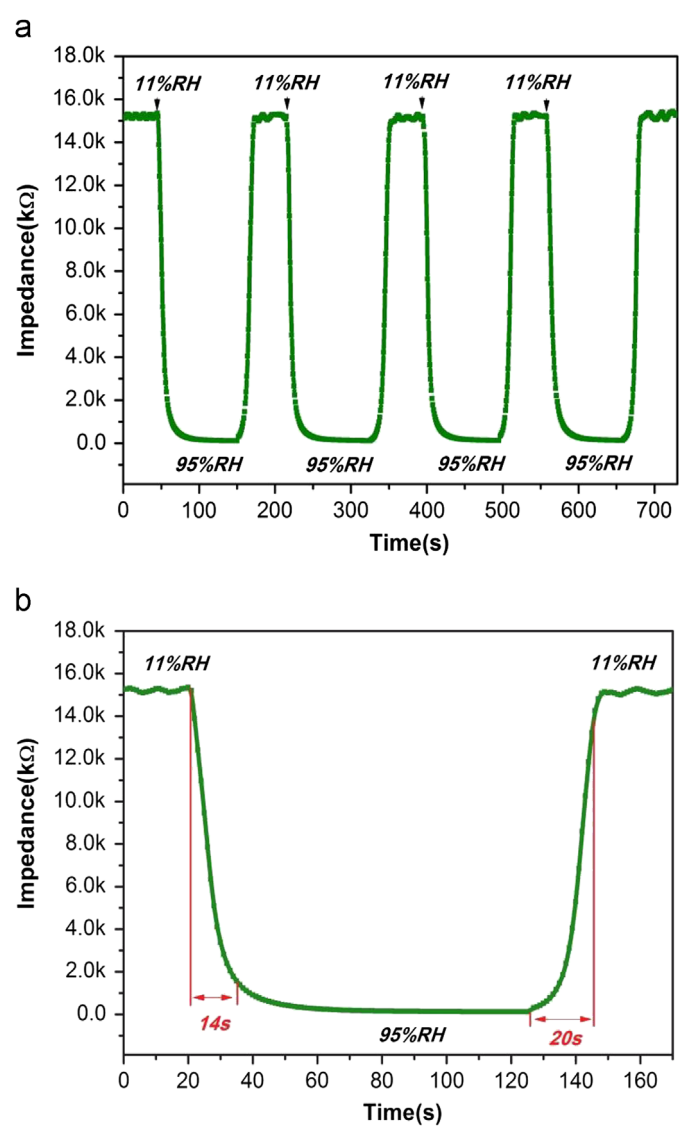

Fig. 9. Response and recovery properties, the test condition was AC 1 V, 100 Hz.

shows the ratio of impedances of the sample at 11 and 98% RH (relative humidity) is larger than 10^3 and the maximum hysteresis of relative humidity is less than 5% RH in the whole humidity range. To check the practicability of the nano-sensor, the response and recovery characteristics are given in Fig. 9. According to the literature [2], the response and recovery times are defined as the time taken to reach 90% of the total impedance change. For this sample, the response time (humidification from 11% to 95% RH) and recovery time (desiccation from 95% to 11% RH) of the sensor are about 14 and 20 s, respectively. Such fast response and recovery behaviors satisfy the requirements for a high-performance humidity sensor.

4. Conclusions

In summary, we have demonstrated a facile approach based on the molten salt reaction for the synthesis of single crystalline $BaTiO_3$ nano-wires. With a relatively higher temperature, appropriate reaction time, and weight ratio of the precursor to KCl salt, large amounts of pure $BaTiO_3$ nano-wires are prepared. The as-synthesized nano-wire displays an average diameter of about 80 nm and a length from tens to several tens of micrometers. Both HRTEM and SAED results show that the nano-wires are single crystalline and grow along [001]. The effects of precursors on the nano-wires growth have been investigated in detail and the proposed growth mechanism based on the self-polarize model has been discussed. Finally, the humidity sensing property of the formed $BaTiO_3$ nano-wire is investigated and the results confirm the obtained nano-wire is a promising high-performance humidity sensor candidate.

Acknowledgments

The authors would like to thank Dr. T. Zhang (Ji-Lin University, Changchun, China) for humidity property analysis. Bao-rang Li is grateful to The National Thermal Power Engineering Technology Research Center for equipment support. This work is also supported by the funds from the National Natural Science Foundation of China (Grant no. 51201064).

References

[1] R.N. Dasw, P. Pramanik, Preparation of nano-crystalline $BaTiO_3$ powders, fibers, and thin films from the same precursor solution, Journal of the American Ceramic Society 93 (2010) 1869–1873.

[2] Y. He, T. Zhang, W. Zheng, R. Wang, X. Liu, Y. Xia, J. Zhao, Humidity sensing properties of BaTiO3 nano-fiber prepared via electro-spinning, Sensors and Actuators B 146 (2010) 98–102.

[3] R. Boucher, P. Renz, C. Li, T. Fuhrlich, J. Bauch, et al., Large coercivity and polarization of sol–gel derived $BaTiO_3$ nano-wires, Journal of Applied Physics 110 (2011) 064112-1–064112-5.

[4] Upendra A. Joshi, Songhak Yoon, Sunggi Baik, Jae Sung, Surfactant-free hydrothermal synthesis of highly tetragonal barium titanate nanowires: a structural investigation, Journal of Physical Chemistry B 110 (2006) 12249–12256.

[5] W. Wang, G. Zhang, Synthesis and optical properties of high-purity CoO nanowires prepared by an environmentally friendly molten salt route, Journal of Crystal Growth 311 (2009) 4275–4280.

[6] C. Lan, J. Gonga, Z. Wang, S. Yang, Synthesis of $K_6Ta_{10.8}O_{30}$ nanowires by molten salt technique, Materials Science and Engineering B 176 (2011) 679–683.

[7] Z. Deng, Y. Dai, W. Chen, X. Pei, Synthesis and characterization of single-crystalline $BaTi_2O_5$ nanowires, Journal of Physical Chemistry C 114 (2010) 1748–1751.

[8] A.C. Santulli, H. Zhou, S. Berweger, M.B. Raschke, E. Sutter, S.S. Wong, Synthesis of single-crystalline one-dimensional $LiNbO_3$ nanowires, Crystal Engineering Communication 12 (2010) 2675–2678.

[9] C. Liu, F. Wang, P. Jia, J. Lin, Z. Zhou, Nanosci, molten salt synthesis and luminescent properties of YVO_4:Ln (Ln=Eu^{3+}, Dy^{3+}) nanophosphors, Journal of Nanoscience and Nanotechnology 12 (2012) 151–158.

[10] J. Ding, C. Deng, W. Yuan, H. Zhu, J. Li, The synthesis of titanium nitride whiskers on the surface of graphite by molten salt media, Ceramics International 39 (2013) 2995–3000.

[11] R. Wu, K. Zhou, Z. Yang, X. Qian, J. Wei, L. Liu, Y. Huang, L. Kong, L. Wang, Molten-salt-mediated synthesis of SiC nanowires for microwave absorption applications, Crystal Engineering Communication 15 (2013) 570–576.

[12] K. Huo, B. Zhu, J. Fu, X. Li, K. Chu Paul, Large-scale synthesis of mullite nanowires by molten salt method, Journal of Nanoscience and Nanotechnology 10 (2010) 4792–4796.

[13] Y. Hayashi, T. Kimura, T. Yamaguchi, Preparation of rod-shaped $BaTiO_3$ powder, Journal of Materials Science 21 (1986) 757–762.

[14] Y.B. Mao, S. Banerjee, S.S. Wong, Large-scale synthesis of single-crystalline perovskite nanostructures, Journal of the American Chemical Society 125 (2003) 15718–15719.

[15] H. Deng, Y.C. Qiu, S.H. Yang, General surfactant-free synthesis of $MTiO_3$ (M: Ba, Sr, Pb) perovskite nano-strips, Journal of Materials Chemistry, 19, 976–982.

[16] K.C. Huang, T.C. Huang, W.F. Hsieh, Morphology-controlled synthesis of barium titanate nano-structures, Inorganic Chemistry 48 (2009) 9180–9184.

[17] P.M. Rørvik, T. Lyngdal, R. Sæterli, Antonius T.J. van Helvoort, R. Holmestad, T. Grande, M.A. Einarsrud, Influence of volatile chlorides on the molten salt synthesis of ternary oxide nano-rods and nanoparticles, Inorganic Chemistry 47 (2008) 3173–3181.

[18] B. Li, X. Wang, M. Yan, L. Li, Preparation and characterization of nano-TiO_2 powder, Materials Chemistry and Physics 78 (2003) 184–188.

[19] B. Roy, S.P. Ahrenkiel, P.A. Fuierer, Controlling the size and morphology of TiO_2 powder by molten and solid salt synthesis, Journal of the American Ceramic Society 91 (2008) 2455–2463.